Characteristics of Microstrip Transmission Lines with High-Dielectric-Constant Substrates

Achintya K. Ganguly and Clifford M. Krowne, *Senior Member, IEEE*

Abstract—**An efficient numerical code is developed from a full-wave analysis in the Fourier transform domain to determine the characteristics of a single-strip or multistrip coplanar transmission line. Modes of both even and odd symmetries are included. The impedance of the transmission line is calculated using the power–current equivalent model. Coupling constants between the even and the odd modes are also calculated. Results are provided for a shielded two-strip coupled microstrip transmission line on high-dielectric-constant substrate such as lanthanum aluminate with applications to superconducting transmission lines.**

I. Introduction

HIGH-TRANSITION-TEMPERATURE (HTC) superconducting materials [1], [2] can be utilized to fabricate shielded microstrip transmission lines with extremely low loss. Recent advances in the techniques to deposit HTC materials such as $YBa_2Cu_3O_{7-x}$ on lanthanum gallate ($LaGaO_3$) [3], [4] and aluminate ($LaAlO_3$) [1] substrates can be effectively used to design single and coupled microstrip transmission lines for operation as low-loss delay lines and filters [5] in the microwave region. These substrates have high dielectric constants ($\epsilon \approx 25$) and small loss tangents (~ 0.001). The available CAD programs for designing delay lines and filters are inaccurate [5] for substrates with dielectric constants greater than 18. Full-wave analysis of the microstrip lines is necessary for accurate modeling of planar transmission lines with high-dielectric-constant substrates.

The spectral decomposition technique in the Fourier transform domain introduced by Itoh and Mitra [6], [7] is a very efficient method for the numerical analysis of planar transmission lines. As shown by Jansen [8], accurate numerical results can be obtained from low-order-determinant eigenvalue equations through a proper choice of basis functions to represent the singular edge behavior of the strip currents. We apply this technique to develop a numerical code to run on CRAY to calculate the dispersion characteristics, the impedances, and the coupling constants of the odd and even modes of a shielded coupled microstrip transmission line. The general equations of the spectral decomposition method are shown in Section II. The numerical results for a coupled two-strip shielded transmission line on lanthanum aluminate substrate are discussed in Section III and the conclusions are given in Section IV.

Manuscript received May 10, 1990; revised March 26, 1991. This work was supported by the Office of Naval Research and the Office of Naval Technology.

The authors are with the Naval Research Laboratory, Washington, DC 20375.

IEEE Log Number 9101011.

II. General Formulation

A cross-sectional view of the configuration under consideration is shown in Fig. 1. It consists of N_s coupled coplanar strips of width $2w$ and uniform spacing s. The strips are infinitely thin and perfectly conducting. The height of the dielectric substrate (region 1) is d_1 and the top layer of height d_2 (region 2) is air. The substrate is assumed to be lossless and nonmagnetic with a relative permittivity ϵ_r. The ground planes of the shielded structure are at $x = \pm a$ and at $y = 0$, $d_1 + d_2$. The unit vectors of the coordinate system will be denoted by $(\hat{e}_x, \hat{e}_y, \hat{e}_z)$. The y axis is perpendicular to the air–dielectric interface, and the z axis is along the direction of wave propagation. We assume that all components of the field and the current density have the same propagation factor $e^{i(\omega t - \beta z)}$, where ω is the frequency and β is the propagation constant of the wave. The vacuum permittivity and permeability will be denoted by ϵ_0 and μ_0, respectively. The calculation of the field relations for planar transmission line structures is a well-established procedure and the details will not be shown. An impedance dyadic Green's function can be derived [7] to express the surface current density $\boldsymbol{J}(x, d_1)$ in terms of the tangential electric field $\boldsymbol{E}(x, d_1)$ satisfying all boundary and interface conditions. The expression in the Fourier transform domain is given by

$$\begin{pmatrix} Z_{zz}(k_n) & Z_{zx}(k_n) \\ Z_{xz}(k_n) & Z_{xx}(k_n) \end{pmatrix} \begin{pmatrix} \pm \tilde{J}_z(k_n, d_1) \\ i\tilde{J}_x(k_n, d_1) \end{pmatrix} = \begin{pmatrix} \mp i\tilde{E}_z(k_n, d_1) \\ \tilde{E}_x(k_n, d_1) \end{pmatrix} \tag{1}$$

where the upper (lower) sign refers to even (odd) modes

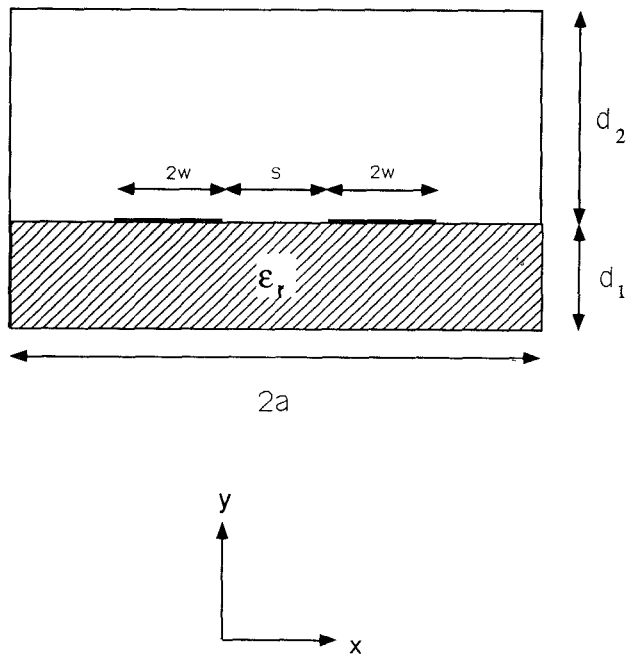

Fig. 1. Cross-sectional view of a coupled microstrip transmission line.

and $\tilde{f}(k_n, d_1)$ is a Fourier transform defined by

$$\tilde{f}(k_n, y) = \frac{1}{(1+\delta_{k_n,0})a}\int_{-a}^{a} f(x,y)\begin{Bmatrix}\cos(k_n x)\\ \sin(k_n x)\end{Bmatrix} dx \quad (2)$$

where $k_n = (2n-1)\pi/2a$ for even modes and $k_n = (n-1)\pi/a$ for odd modes (n being a nonzero positive integer) and $\delta_{k_n,0}$ is the Kronecker delta. The cosine or the sine Fourier transform in (2) will be used depending on whether $f(x,y)$ is an even or an odd function of x. The elements Z_{ij} are given by

$$Z_{xx}(k_n) = \left(k_n^2 Z_e - \beta^2 Z_h\right)/\left(k_n^2+\beta^2\right) \quad (3)$$

$$Z_{zz}(k_n) = \left(\beta^2 Z_e - k_n^2 Z_h\right)/\left(k_n^2+\beta^2\right) \quad (4)$$

$$Z_{xz}(k_n) = Z_{zx}(k_n) = \beta k_n (Z_e + Z_h)/\left(k_n^2+\beta^2\right) \quad (5)$$

where Z_e and Z_h are the impedances, defined by

$$Z_e = Z_0 \bar{Z}_e = Z_0/\left(\bar{Y}_1^e + \bar{Y}_2^e\right)$$

and

$$Z_h = Z_0 \bar{Z}_h = Z_0/\left(\bar{Y}_1^h + \bar{Y}_2^h\right). \quad (6)$$

In (6), $Z_0 = \sqrt{\mu_0/\epsilon_0}$ is the vacuum impedance and $\bar{Y}_p^h$ and $\bar{Y}_p^e$ ($p = 1,2$) are, respectively, the normalized characteristic admittances of the LSE and LSM modes in regions 1 and 2, given by

$$\bar{Y}_1^h = \frac{\Gamma_1}{k_0}\coth(\Gamma_1 d_1) \quad \text{and} \quad \bar{Y}_2^h = \frac{\Gamma_2}{k_0}\coth(\Gamma_2 d_2) \quad (7)$$

$$\bar{Y}_1^e = \frac{\epsilon_r k_0}{\Gamma_1}\coth(\Gamma_1 d_1) \quad \text{and} \quad \bar{Y}_2^e = \frac{k_0}{\Gamma_2}\coth(\Gamma_2 d_2) \quad (8)$$

where $k_0 = \sqrt{\mu_0\epsilon_0}\,\omega$ and

$$\Gamma_1 = \left\{k_n^2 + \beta^2 - \epsilon_r k_0^2\right\}^{1/2}$$

$$\Gamma_2 = \left\{k_n^2 + \beta^2 - k_0^2\right\}^{1/2}. \quad (9)$$

$\Gamma_{1,2}$ may be real or imaginary. For imaginary Γ, we should replace Γ by $i\Gamma$, $\sinh\Gamma$ by $i\sin\Gamma$, and $\cosh\Gamma$ by $\cos\Gamma$ in (7)–(9) and in all subsequent equations.

It is to be noted that the current density $\boldsymbol{J}(x, d_1)$ and the tangential electric field $\boldsymbol{E}(x, d_1)$ are nonzero in the complementary regions of the domain $-a < x < a$. Hence, a determinantal form of a dispersion equation can be obtained by eliminating E_x and E_z from (1) with a Galerkin-like approach [7] in the Fourier transform domain by expanding the strip currents in terms of suitable basis functions given in Appendix I. On substituting (A18) in (1), we take the inner product with the basis functions $\tilde{\chi}_p(k_n)$ and $\tilde{\zeta}_p(k_n)$ for all p and obtain the following matrix equation [7]:

$$\sum_{m=1}^{M} K_{zz}^{pm} A_m + \sum_{m=1}^{N} K_{zx}^{pm} B_m = 0,$$

$$p = 1,2,\cdots, M = m_z N_s$$

$$\sum_{m=1}^{M} K_{xz}^{pm} A_m + \sum_{m=1}^{N} K_{xx}^{pm} B_m = 0,$$

$$p = 1,2,\cdots, N = m_x N_s \quad (10)$$

where the elements K_{mn}^{pq} are given by

$$K_{zz}^{pm} = \sum_{n=1}^{\infty} Z_{zz}(k_n)\tilde{\chi}_p(k_n)\tilde{\chi}_m(k_n)$$

$$K_{zx}^{pm} = \sum_{n=1}^{\infty} Z_{zx}(k_n)\tilde{\chi}_p(k_n)\tilde{\zeta}_m(k_n)$$

$$K_{xz}^{pm} = \sum_{n=1}^{\infty} Z_{xz}(k_n)\tilde{\zeta}_p(k_n)\tilde{\chi}_m(k_n)$$

$$K_{xx}^{pm} = \sum_{n=1}^{\infty} Z_{xx}(k_n)\tilde{\zeta}_p(k_n)\tilde{\zeta}_m(k_n). \quad (11)$$

Equations (10) and (11) involve only real quantities for propagation in a lossless medium. The set of equations (10) are solved for the propagation constant β by setting its determinant of order $(M+N)\times(M+N)$ equal to zero. On substitution of β in (10), all coefficients A_m and B_m can be determined in terms of one coefficient (largest in magnitude) from the solution of $(M+N-1)$ simultaneous equations obtained from (10) by eliminating one row from the matrix. The remaining unknown coefficient may be calculated from the power in the transmission line. The field and the current density components can be calculated by substituting the coefficients A_p and B_p in the expressions shown in Appendixes I and II.

The characteristics of the transmission line can be obtained from the propagation constant, the longitudinal current in the strip, and the power flow in the circuit. We are mainly interested in the propagation of the funda-

mental mode, which is TEM-like in character. For these modes, the power–current equivalent model seems to be the most suitable one [9]–[12] for modeling interconnections between microstrip lines and such TEM structures as loads and drivers. The total average power in each eigenmode of the transmission line propagating in the z direction can be calculated by integrating the axial component of Poynting's vector over the cross section of the transmission line:

$$P_{\text{av}} = \frac{1}{2}\text{Re}\left[\int_{-a}^{a}\int_{0}^{d_1+d_2} \boldsymbol{E}\times\boldsymbol{H}^*\cdot\hat{e}_z\,dx\,dy\right]. \quad (12)$$

We assume that the total power has the following distribution over the N_s strips, as proposed by Jansen [8]:

$$P_{j,\text{av}} = \frac{1}{2}\text{Re}\left[\int_{-a}^{a}\int_{0}^{d_1+d_2} \boldsymbol{E}\times\boldsymbol{H}_j^*\cdot\hat{e}_z\,dx\,dy\right] \quad (13)$$

where $P_{j,\text{av}}$ is the power contributed by the jth strip, $\boldsymbol{H}_j$ is the magnetic field excited by the current in the jth strip, and $\boldsymbol{E}$ is the total electric field from all the strips. The impedance associated with the jth strip is defined by

$$Z_j = \frac{P_{j,\text{av}}}{I_{j,\text{av}}^2} = \frac{2P_{j,\text{av}}}{\text{Re}\left[I_j I_j^*\right]} \quad (14)$$

where I_j is the longitudinal component of the current in the jth strip, given by

$$I_j = \left[\int_{x_j-w}^{x_j+w} J_{z,j}(x,d_1)\,dx\right]e^{i(\omega t-\beta z)}. \quad (15)$$

Substituting (A1), (A3)–(A6), and (A12) in (15), we get

$$I_j(z,t) = e^{i(\omega t-\beta z)}\begin{cases}\dfrac{(1+\delta_{j,0})\pi w\hat{A}}{2}\displaystyle\sum_{m=1}^{m_z}\bar{a}_{j,m}J_0((m-1)\pi) & \text{(even mode)}\\ -\dfrac{\pi w\hat{A}}{2}\displaystyle\sum_{m=1}^{m_z}\bar{b}_{j,m}J_0((m-1)\pi) & \text{(odd mode)}.\end{cases} \quad (16)$$

In the case of odd modes, $I_j = 0$ for $j = 0$ and the definition of impedance in (14) does not apply to the odd modes on the center strip at $x = 0$. From (12)–(14), it is evident that the total power in the circuit is

$$P_{\text{av}} = \sum_{j=1}^{N_s} Z_j I_{j,\text{av}}^2. \quad (17)$$

The explicit expression for $P_{j,\text{av}}$ can be derived by substituting (A18)–(A20), and (A23)–(A26) in (13):

$$P_{j,\text{av}} = \frac{Z_0\hat{A}^2 aD\beta}{4k_0}\sum_{n=1}^{\infty}(1+\delta_{k_n,0})\cdot\left(\bar{P}_{1n}\bar{J}_{xn}\bar{J}_{xj}(n) + \bar{P}_{2n}\bar{J}_{zn}\bar{J}_{zj}(n) + \bar{P}_{3n}\bar{J}_{xn}\bar{J}_{zj}(n) + \bar{P}_{4n}\bar{J}_{zn}\bar{J}_{xj}(n)\right) \quad (18)$$

where D is an arbitrary normalizing length, which may be chosen as the total height of the shielded transmission line, i.e., $D = d_1 + d_2 = h$. The dimensionless quantities $\bar{P}_{jn}$ are given by

$$\bar{P}_{1n} = \left[\alpha_{nz}^2\bar{Z}_h^2\left(\frac{d_1}{D}\psi_1^- + \frac{d_2}{D}\psi_2^-\right) + \alpha_{nx}^2\bar{Z}_e^2\left(\frac{\epsilon_r k_0^2}{\Gamma_1^2}\frac{d_1}{D}\psi_1^+ + \frac{k_0^2}{\Gamma_2^2}\frac{d_2}{D}\psi_2^+\right) - 2\alpha_{nx}^2\bar{Z}_h\bar{Z}_e\frac{\left(\bar{Y}_2^e + \bar{Y}_1^e/\epsilon_r\right)}{k_0 D}\right]$$

$$\bar{P}_{2n} = \left[\alpha_{nx}^2\bar{Z}_h^2\left(\frac{d_1}{D}\psi_1^- + \frac{d_2}{D}\psi_2^-\right) + \alpha_{nz}^2\bar{Z}_e^2\left(\frac{\epsilon_r k_0^2}{\Gamma_1^2}\frac{d_1}{D}\psi_1^+ + \frac{k_0^2}{\Gamma_2^2}\frac{d_2}{D}\psi_2^+\right) + 2\alpha_{nx}^2\bar{Z}_h\bar{Z}_e\frac{\left(\bar{Y}_2^e + \bar{Y}_1^e/\epsilon_r\right)}{k_0 D}\right]$$

$$\bar{P}_{3n} = \alpha_{nx}\alpha_{nz}\left[\bar{Z}_e^2\left(\frac{\epsilon_r k_0^2}{\Gamma_1^2}\frac{d_1}{D}\psi_1^+ + \frac{k_0^2}{\Gamma_2^2}\frac{d_2}{D}\psi_2^+\right) - \bar{Z}_h^2\left(\frac{d_1}{D}\psi_1^- + \frac{d_2}{D}\psi_2^-\right)\right] + 2\alpha_{nx}^2\bar{Z}_h\bar{Z}_e\frac{k_n\left(\bar{Y}_2^e + \bar{Y}_1^e/\epsilon_r\right)}{\beta k_0 D}$$

$$\bar{P}_{4n} = \alpha_{nx}\alpha_{nz}\left[\bar{Z}_e^2\left(\frac{\epsilon_r k_0^2}{\Gamma_1^2}\frac{d_1}{D}\psi_1^+ + \frac{k_0^2}{\Gamma_2^2}\frac{d_2}{D}\psi_2^+\right) - \bar{Z}_h^2\left(\frac{d_1}{D}\psi_1^- + \frac{d_2}{D}\psi_2^-\right)\right] - 2\alpha_{nz}^2\bar{Z}_h\bar{Z}_e\frac{k_n\left(\bar{Y}_2^e + \bar{Y}_1^e/\epsilon_r\right)}{\beta k_0 D} \quad (19)$$

where $\alpha_{nz} = \beta/\{k_n^2+\beta^2\}^{1/2}$, $\alpha_{nx} = k_n/\{k_n^2+\beta^2\}^{1/2}$, and

$$\psi_1^{\pm} = \frac{\coth(\Gamma_1 d_1)}{\Gamma_1 d_1} \pm \frac{1}{\sinh^2(\Gamma_1 d_1)}$$

$$\psi_2^{\pm} = \frac{\coth(\Gamma_2 d_2)}{\Gamma_2 d_2} \pm \frac{1}{\sinh^2(\Gamma_2 d_2)}. \quad (20)$$

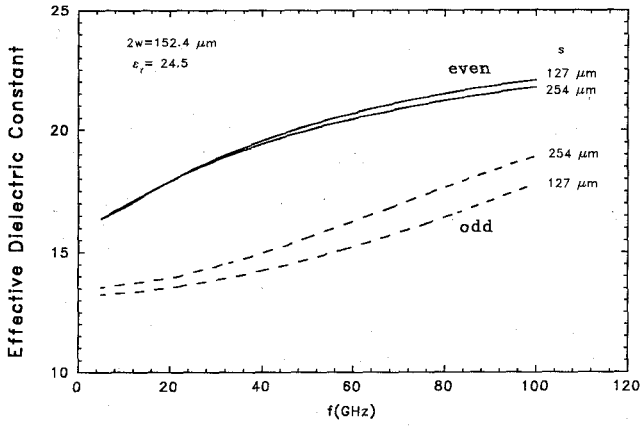

Fig. 2. Effective dielectric constant versus frequency for $s = 127.0$ and 254.0 μm. The solid and the dashed curves represent the even and odd modes, respectively. Other parameters are $\epsilon_r = 24.5$, $2w = 152.4$ mm, $2a = 0.254$ cm, $d_2 = 0.254$ cm, and $d_1 = 0.0254$ cm.

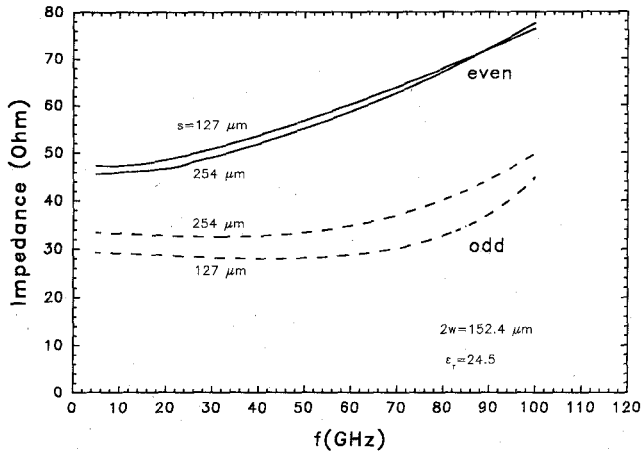

Fig. 3. Plot of impedance as function of frequency for the same parameters as in Fig. 1.

The normalized Fourier transforms of the strip current components in (18) are defined in (A18) and (A19).

III. Results

In this paper, we show the results of the numerical computation of the propagation characteristics of the lowest even and odd modes of a two-strip coupled, shielded microstrip transmission line. The propagation characteristics depend on a large number of parameters such as f, d_1, d_2, a, w, s, and ϵ. Here, we show the variation of the characteristics with certain of these parameters, e.g. frequency (f), width ($2w$), and separation (s) of the two strips. The other parameters are kept fixed and we choose $d_1 = 0.0254$ cm, $d_2 = 0.254$ cm, $2a = 0.254$ cm, and $\epsilon_r = 24.5$. The dielectric constant refers to the lanthanum aluminate substrate. The numerical calculations are performed by truncating the infinite sum in the spectral decomposition (eq. (11)) to a finite number $n_{\max}$, and the number of the basis functions for the x and z

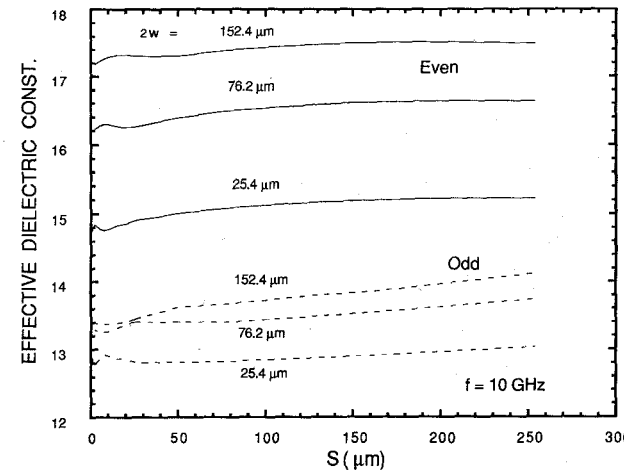

Fig. 4. Effective dielectric constant versus separation of the strips (s) at $f = 10$ GHz for $2w = 25.4$ μm, 76.2 μm, and 152.4 μm. Also, $\epsilon_r = 24.5$, $2a = 0.254$ cm, $d_2 = 0.254$ cm, and $d_1 = 0.0254$ cm.

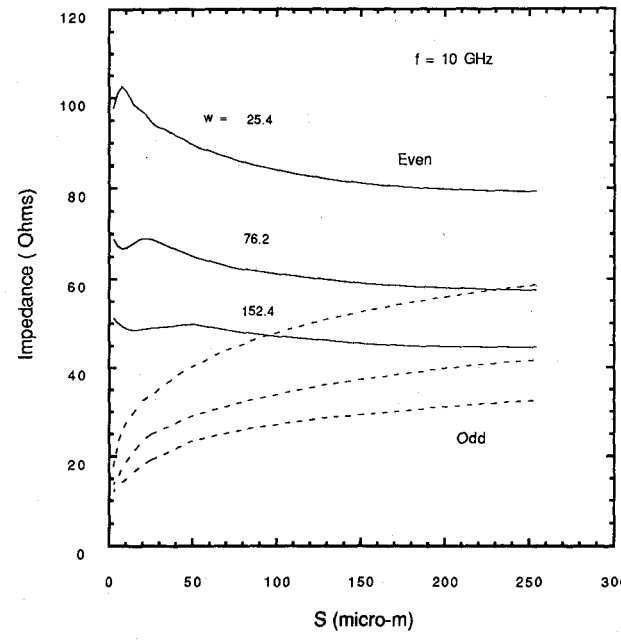

Fig. 5. Impedance versus strip separation for the same parameters as in Fig. 4. The solid curves are for even modes and the dashed curves are for odd modes.

components of the strip currents are truncated to m_x and m_z, respectively. Calculations show that the choice $n_{\max} = 300$, $m_z = 3$, and $m_x = 3$ provides an accuracy of 1 part in 10^4. It should be noted that $\xi_{11}(x) \neq 0$ but $\eta_{11}(x) = 0$ (eqs. (A3) and (A4)) for the even modes and considering $\eta_{11}(x)$ as a basis function may seem unnecessary. However, numerical instability for the coupled striplines occurs if $\xi_{1m}(x)$ and $\eta_{1m}(x)$ are not correctly paired.

The effective dielectric constants (ϵ_{eff}) of the even and odd symmetry modes are shown in Fig. 2 as functions of frequency for two values of s (strip separation) with $2w = 152.4$ μm. As expected, ϵ_{eff} increases with frequency and is more sensitive to s at higher frequency. As

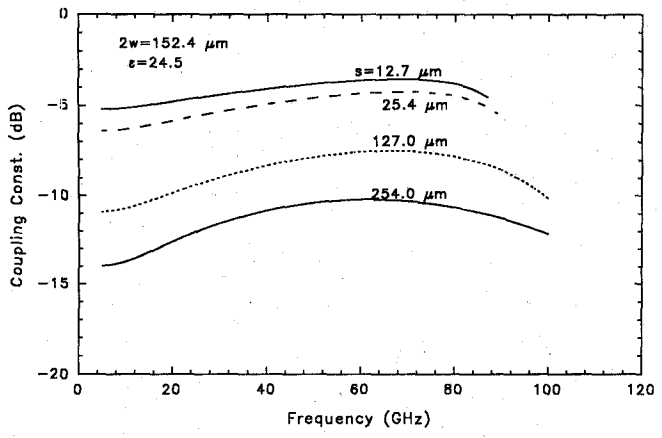

Fig. 6. Variation of the coupling constant between the even and odd modes with frequency for four values of strip separation $s = 12.7$ μm, 25.4 μm, 127.0 μm, and 254.0 μm and $\epsilon_r = 24.5$, $2a = 0.254$ cm, $d_2 = 0.254$ cm, and $d_1 = 0.0254$ cm.

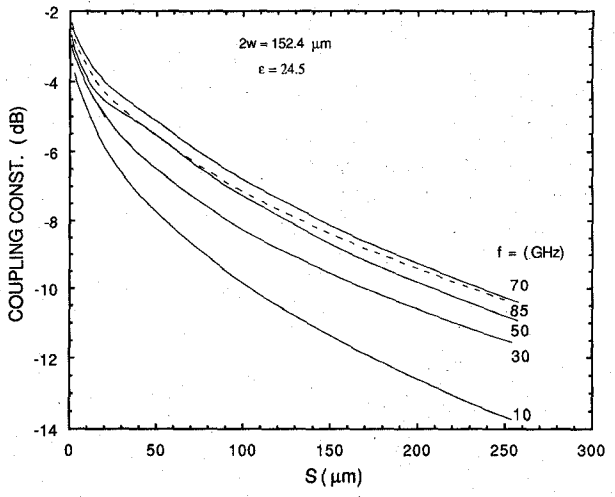

Fig. 7. Coupling constant versus strip separation at $f = 10$, 30, 50, 70, and 85 GHz. Other parameters are the same as in Fig. 6.

the separation of the strips increases, the effective dielectric constants for the even modes decrease while those for the odd modes increase. The variation of the impedance (Z) with frequency is plotted in Fig. 3 for the same parameters as in Fig. 2. In general, the impedance increases with frequency. Two opposing factors contribute to the dependence of the impedance on frequency. The effective dielectric constant increases but the effective width of the strips decreases with frequency. At high frequencies, the second factor dominates, resulting in an increase in impedance. At low frequencies, the two effects are nearly equal and the impedance is practically independent of frequency. For the odd modes, a small decrease in impedance occurs at low frequency. Since the electric field lines for the odd modes run also between the strips, the effective width of the strips does not decrease with frequency as rapidly as in the case of the even modes.

The dependence of ϵ_{eff} and Z on the strip separation is shown in detail in Figs. 4 and 5, respectively at $f = 10$ GHz for three different strip widths. For both even and odd modes, ϵ_{eff} shows oscillatory behavior at very small values of s and then changes very slowly as s increases. The region of the oscillatory behavior decreases as the width of the strip decreases. The impedance of the even modes, also, shows oscillations at small s opposite to that for ϵ_{eff} and then slowly decreases with an increase in s. The impedance for the odd modes always increases with the strip separation. For both types of modes, the effective dielectric constant increases and the impedance decreases with an increase in the strip width.

The coupling constant between the even and the odd modes of the coupled transmission line is shown in Figs. 6 and 7. These parameters are important for designing filters. The coupling constant is defined by $K = (\beta_{\text{ev}} Z_{\text{ev}} - \beta_{\text{od}} Z_{\text{od}})/(\beta_{\text{ev}} Z_{\text{ev}} + \beta_{\text{od}} Z_{\text{od}})$, where the subscripts "ev" and "od" denote even and odd modes, respectively. Fig. 6 shows the variation of the coupling constant with frequency for different separations between the strips. The coupling loss as a function of frequency passes through a minimum at each s. The minimum loss increases but the corresponding frequency decreases with an increase in s. For $s = 12.7$ μm, the minimum coupling loss of -3.9 dB occurs at $f = 70$ GHz whereas the minimum coupling loss is -10.5 dB at $f = 60$ GHz when $s = 254.0$ μm. In Fig. 7, the coupling constant is plotted as a function of s for different frequencies. At each frequency the coupling loss increases with an increase in the strip separation but for a fixed strip separation the coupling loss first decreases and then increases as the frequency is increased.

IV. Conclusions

We have developed an efficient numerical code for calculating the propagation characteristics of single and coupled microstrip transmission lines from a full-wave analysis in the Fourier transform domain. The numerical code is applicable to transmission lines with high-dielectric-constant substrate. The code will be very useful in designing extremely low loss delay lines and filters fabricated with high-temperature superconducting strips on lanthanum aluminate or gallate substrate. In high-dielectric-constant substrates, the effective dielectric constant and the impedance of the coupled transmission lines show oscillatory behavior with changes in strip separation when the separation is very small. Such small separations should be avoided in the design of delay lines and filters.

Appendix I

A suitable set of basis functions satisfying the edge conditions term by term is required to represent the strip current components for efficient numerical computation. For this purpose we choose the set of basis functions proposed by Jansen [8] to express the current distribution for a planar transmission line with N_s symmetrically placed strips [13], [14]. For the even modes, we may write (sup-

pressing the propagation factor $e^{i(\omega t-\beta z)}$)

$$J_z(x,d_1)=\sum_j J_{z,j}(x,d_1)=\frac{1}{2}\sum_{\substack{j=-n_s\\ j\neq 0}}^{n_s}\sum_{m=1}^{m_z}\{a_{jm}\xi_{1m}(x-x_j)-b_{jm}\xi_{2m}(x-x_j)\}+\left[\sum_{m=1}^{m_1}a_{0m}\xi_{1m}(x)\right]$$

$$iJ_x(x,d_1)=\sum_j iJ_{x,j}(x,d_1)=\frac{1}{2}\sum_{\substack{j=-n_s\\ j\neq 0}}^{n_s}\sum_{m=1}^{m_x}\{c_{jm}\eta_{1m}(x-x_j)+d_{jm}\eta_{2m}(x-x_j)\}+\left[\sum_{m=1}^{m_z}c_{0m}\eta_{1m}(x)\right] \tag{A1}$$

where $n_s=(N_s-1)/2$ or $N_s/2$ for odd or even number of strips, respectively and m_x and m_z are the number of basis functions for J_x and J_z. The distance of the center of the jth strip from the origin is denoted by x_j. For symmetrically placed strips, we have

$$x_j=\begin{cases} j(s+2w), \\ \quad j=0,\pm 1,\pm 2,\cdots,\pm n_s & (N_s \text{ odd}) \\ \pm\left[(|j|-\frac{1}{2})(s+2w)\right], \\ \quad j=\pm 1,\pm 2,\cdots,\pm n_s & (N_s \text{ even}). \end{cases} \tag{A2}$$

The terms in square brackets in (A1) are to be included only if N_s is odd where $j=0$ is the center strip located at the origin. The quantities ξ_{1m} and ξ_{2m} are single-strip even and odd basis functions for J_z while η_{1m} and η_{2m} are the odd and even basis functions for J_x, which are given by

$$\xi_{1m}(x)=\begin{cases}\dfrac{\cos((m-1)\pi x/w)}{\{1-(x/w)^2\}^{1/2}}, & |x|\leqslant w \\ 0, & w<|x|<a\end{cases} \tag{A3}$$

$$\eta_{1m}(x)=\begin{cases}\dfrac{\sin((m-1)\pi x/w)}{\{1-(x/w)^2\}^{1/2}}, & |x|\leqslant w \\ 0, & w<|x|<a\end{cases} \tag{A4}$$

$$\xi_{2m}(x)=\begin{cases}\dfrac{\sin((m-\frac{1}{2})\pi x/w)}{\{1-(x/w)^2\}^{1/2}}, & |x|\leqslant w \\ 0, & w<|x|<a\end{cases} \tag{A5}$$

$$\eta_{2m}(x)=\begin{cases}\dfrac{\cos((m-\frac{1}{2})\pi x/w)}{\{1-(x/w)^2\}^{1/2}}, & |x|\leqslant w \\ 0, & w<|x|<a.\end{cases} \tag{A6}$$

In (A4), $\eta_{11}(x)=0$, but we keep this function for the proper pairing of ξ_{1m} and η_{1m} to avoid numerical instability. From (2), the Fourier transforms of the basis functions in (A3)–(A6) are given, respectively, by

$$\tilde{\xi}_{1m}(k_n)=\frac{\pi w}{(1+\delta_{k_n,0})2a}\cdot\left[J_0(k_nw-(m-1)\pi)+J_0(k_nw+(m-1)\pi)\right]$$

$$\tilde{\eta}_{1m}(k_n)=\frac{\pi w}{(1+\delta_{k_n,0})2a}\cdot\left[J_0(k_nw-(m-1)\pi)-J_0(k_nw+(m-1)\pi)\right]$$

$$\tilde{\xi}_{2m}(k_n)=\frac{\pi w}{(1+\delta_{k_n,0})2a}\cdot\left[J_0(k_nw-(m-\tfrac{1}{2})\pi)-J_0(k_nw+(m-\tfrac{1}{2})\pi)\right]$$

$$\tilde{\eta}_{2m}(k_n)=\frac{\pi w}{(1+\delta_{k_n,0})2a}\cdot\left[J_0(k_nw-(m-\tfrac{1}{2})\pi)+J_0(k_nw+(m-\tfrac{1}{2})\pi)\right]. \tag{A7}$$

From the symmetry properties of the even modes $J_z(-x)=J_z(x)$ and $J_x(-x)=-J_x(x)$, it follows that $a_{-jm}=a_{jm}$, $b_{-jm}=-b_{jm}$, $c_{-jm}=c_{jm}$, and $d_{-jm}=-d_{jm}$ and we can express the current density components as a sum over the strips with $x_j\geqslant 0$:

$$J_z(x,d_1)=\frac{1}{2}\sum_{j=1}^{n_s}\sum_{m=1}^{m_z}\{a_{jm}(\xi_{1m}(x-x_j)+\xi_{1m}(x+x_j))-b_{jm}(\xi_{2m}(x-x_j)-\xi_{2m}(x+x_j))\}+\left[\sum_{m=1}^{m_z}a_{0m}\xi_{1m}(x)\right] \tag{A8}$$

$$iJ_x(x,d_1)=\frac{1}{2}\sum_{j=1}^{n_s}\sum_{m=1}^{m_x}\{c_{jm}(\eta_{1m}(x-x_j)+\eta_{1m}(x+x_j))+d_{jm}(\eta_{2m}(x-x_j)-\eta_{2m}(x+x_j))\}+\left[\sum_{m=1}^{m_z}c_{0m}\eta_{1m}(x)\right] \tag{A9}$$

where the terms inside the square brackets are included if N_s is odd. From (2), the Fourier transforms of $J_z(x,d)$ and $J_x(x,d)$ are, respectively, given by

$$\tilde{J}_z(k_n,d_1)=\left[\sum_{m=1}^{m_z}a_{0m}\tilde{\xi}_{1m}(k_n)\right]+\sum_{j=1}^{n_s}\sum_{m=1}^{m_z}\{a_{jm}\tilde{\xi}_{1m}(k_n)\cdot\cos(k_nx_j)+b_{jm}\tilde{\xi}_{2m}(k_n)\sin(k_nx_j)\} \tag{A10}$$

$$i\tilde{J}_x(k_n,d_1)=\left[\sum_{m=1}^{m_z}c_{0m}\tilde{\eta}_{1m}(k_n)\right]+\sum_{j=1}^{n_s}\sum_{m=1}^{m_x}\{c_{jm}\tilde{\eta}_{1m}(k_n)\cdot\cos(k_nx_j)+d_{jm}\tilde{\eta}_{2m}(k_n)\sin(k_nx_j)\}. \tag{A11}$$

As before, the terms in square bracket in (A10) and (A11)

are to be included when N_s is odd and refer to the strip with its center at the origin ($j = 0$).

Since the symmetry for the odd modes is given by $J_z(-x) = -J_z(x)$ and $J_x(-x) = J_x(x)$, we may use the following expansions to represent J_z and J_x for these modes:

$$-J_z(x,d_1) = \frac{1}{2}\sum_{j=1}^{n_s}\sum_{m=1}^{m_z}\left\{a_{jm}\left(\xi_{2m}(x-x_j)+\xi_{2m}(x+x_j)\right) + b_{jm}\left(\xi_{1m}(x-x_j)-\xi_{1m}(x+x_j)\right)\right\} + \left[\sum_{m=1}^{m_z} a_{0m}\xi_{2m}(x)\right] \quad \text{(A12)}$$

$$iJ_x(x,d_1) = \frac{1}{2}\sum_{j=1}^{n_s}\sum_{m=1}^{m_x}\left\{c_{jm}\left(\eta_{2m}(x-x_j)+\eta_{2m}(x+x_j)\right) - d_{jm}\left(\eta_{1m}(x-x_j)-\eta_{1m}(x+x_j)\right)\right\} + \left[\sum_{m=1}^{m_x} c_{0m}\eta_{2m}(x)\right] \quad \text{(A13)}$$

with the following Fourier transforms:

$$-\tilde{J}_z(k_n,d_1) = \left[\sum_{m=1}^{m_z} a_{0m}\tilde{\xi}_{2m}(k_n)\right] + \sum_{j=1}^{n_s}\sum_{m=1}^{m_z}\left\{a_{jm}\tilde{\xi}_{2m}(k_n)\cdot\cos(k_n x_j) + b_{jm}\tilde{\xi}_{1m}(k_n)\sin(k_n x_j)\right\} \quad \text{(A14)}$$

$$i\tilde{J}_x(k_n,d_1) = \left[\sum_{m=1}^{m_x} c_{0m}\tilde{\eta}_{2m}(k_n)\right] + \sum_{j=1}^{n_s}\sum_{m=1}^{m_x}\left\{c_{jm}\tilde{\eta}_{2m}(k_n)\cdot\cos(k_n x_j) + d_{jm}\tilde{\eta}_{1m}(k_n)\sin(k_n x_j)\right\}. \quad \text{(A15)}$$

To develop a concise notation, we introduce two sets of generalized basis functions, $\tilde{\chi}_p(k_n)$ and $\tilde{\zeta}_p(k_n)$, of dimensions $M = m_z n_s$ and $N = m_x n_s$, respectively. For the even modes, the set $\tilde{\chi}_p$ is formed by arranging the elements $\cdots, \tilde{\xi}_{1m}\cos(k_n x_j), \cdots, \tilde{\xi}_{2m}\sin(k_n x_j), \cdots$ from (A10) in ascending orders first in the index m and then in the index j; the set $\tilde{\zeta}_p$ is similarly formed from the elements $\cdots, \tilde{\eta}_{2m}\cos(k_n x_j), \cdots, \tilde{\eta}_{1m}\sin(k_n x_j), \cdots$ in (A11). Thus, we may write for the even modes

$$\tilde{\chi}_p(k_n) = \left[\cdots, \tilde{\xi}_{1m}(k_n)\cos(k_n x_j), \cdots, \tilde{\xi}_{2m}(k_n)\sin(k_n x_j), \cdots\right]$$
$$\tilde{\zeta}_q(k_n) = \left[\cdots, \tilde{\eta}_{1l}(k_n)\cos(k_n x_j), \cdots, \tilde{\eta}_{2l}(k_n)\sin(k_n x_j), \cdots\right] \quad \text{(A16)}$$

where $p = 1,2,\cdots,M$, $m = 1,2,\cdots,m_z$, $q = 1,2,\cdots,N$, $l = 1,2,\cdots,m_x$, and $j = [0],1,2,\cdots,n_s$. The term with $j = 0$ occurs for N_s odd only. From (A14) and (A15), the generalized basis functions for the odd modes may similarly be written as

$$\tilde{\chi}_p(k_n) = \left[\cdots, \tilde{\xi}_{2m}(k_n)\cos(k_n x_j), \cdots, \tilde{\xi}_{1m}(k_n)\sin(k_n x_j), \cdots\right]$$
$$\tilde{\zeta}_q(k_n) = \left[\cdots, \tilde{\eta}_{2l}(k_n)\cos(k_n x_j), \cdots, \tilde{\eta}_{1l}(k_n)\sin(k_n x_j), \cdots\right] \quad \text{(A17)}$$

where the indices p, q, m, l, and j have the same range as in (A14). In conformity with the above notation, we combine the expansion coefficients $a_{jm},\cdots,b_{jm}$ into a set A_p (dimension M) and the coefficients $c_{jl},\cdots,d_{jl}$ into another set B_q (dimension N). Thus, (A10), (A11) and (A14), (A15) for the strip currents in the Fourier transform domain assume the forms

$$\pm\tilde{J}_z(k_n,d_1) = \sum_{p=1}^{M} A_p\tilde{\chi}_p(k_n) = \hat{A}\sum_{p=1}^{M}\bar{A}_p\tilde{\chi}(k_n) = \hat{A}\bar{J}_{zn}$$
$$i\tilde{J}_x(k_n,d_1) = \sum_{p=1}^{N} B_p\tilde{\zeta}_p(k_n) = \hat{A}\sum_{p=1}^{N}\bar{B}_p\tilde{\zeta}(k_n) = \hat{A}\bar{J}_{xn} \quad \text{(A18)}$$

where $\bar{A}_p = A_p/\hat{A}$, $\bar{B}_p = B_p/\hat{A}$, and $\hat{A}$ is the largest (in magnitude) element of the set of coefficients A_p, B_p. In (A18), $\bar{J}_{zn}$ and $\bar{J}_{xn}$ are the normalized Fourier transforms of the strip current components from all the strips. For later use, we also define the normalized Fourier transforms of the strip current components associated with a particular (jth) strip. For the even modes, we have

$$\bar{J}_{z,j}(n) = \frac{(1+\delta_{j,0})}{2}\sum_{m=1}^{m_z}\left(\bar{a}_{jm}\tilde{\xi}_{1m}(k_n)\cos(k_n x_j) + \bar{b}_{jm}\tilde{\xi}_{2m}(k_n)\sin(k_n x_j)\right)$$
$$\bar{J}_{x,j}(n) = \frac{(1+\delta_{j,0})}{2}\sum_{m=1}^{m_x}\left(\bar{c}_{jm}\tilde{\eta}_{1m}(k_n)\cos(k_n x_j) + \bar{d}_{jm}\tilde{\eta}_{2m}(k_n)\sin(k_n x_j)\right) \quad \text{(A19)}$$

and for odd modes

$$\bar{J}_{z,j}(n) = \frac{(1+\delta_{j,0})}{2}\sum_{m=1}^{m_z}\left(\bar{a}_{jm}\tilde{\xi}_{2m}(k_n)\cos(k_n x_j) + \bar{b}_{jm}\tilde{\xi}_{1m}(k_n)\sin(k_n x_j)\right)$$
$$\bar{J}_{x,j}(n) = \frac{(1+\delta_{j,0})}{2}\sum_{m=1}^{m_x}\left(\bar{c}_{jm}\tilde{\eta}_{2m}(k_n)\cos(k_n x_j) + \bar{d}_{jm}\tilde{\eta}_{1m}(k_n)\sin(k_n x_j)\right) \quad \text{(A20)}$$

where $\bar{a}_{jm} = a_{jm}/\hat{A}$, $\bar{b}_{jm} = b_{jm}/\hat{A}$, $\bar{c}_{jm} = c_{jm}/\hat{A}$, and $\bar{d}_{jm}$

$= d_{jm}/\hat{A}$. It should be noted that there is a one to one correspondence between the elements a_{jm}, b_{jm} and A_p as well as between c_{jm}, d_{jm} and B_q.

Appendix II

For the sake of completeness, we give the expressions for the electric ($\boldsymbol{E}$) and magnetic ($\boldsymbol{H}$) field components used in the calculation of the power flow in the circuit. The hybrid field components in the microstrip transmission line can be expressed as a superposition of the complete set of LSE (TE to y) and LSM (TM to y) modes of a dielectrically loaded waveguide. The field structures of the LSE and the LSM modes can be derived from the two scalar potentials [15] $\psi^h(x,y,z,t)$ and $\psi^e(x,y,z,t)$, respectively. Since we are considering only propagating waves with angular frequency ω and propagation constant β, we may assume the following forms for the scalar potentials:

$$\psi^h = e^{i(\omega t-\beta z)}\begin{cases} i\sum_{n=1}^{\infty} A_n^h \begin{Bmatrix}\sin(k_n x)\\ \cos(k_n x)\end{Bmatrix} \sinh(\Gamma_1 y), & 0 < y \leqslant d_1 \\ i\sum_{n=1}^{\infty} B_n^h \begin{Bmatrix}\sin(k_n x)\\ \cos(k_n x)\end{Bmatrix} \sinh(\Gamma_2(h-y)), & d_1 < y \leqslant d_1 + d_2 = h \end{cases} \tag{A21}$$

and

$$\psi^e = e^{i(\omega t-\beta z)}\begin{cases} i\sum_{n=1}^{\infty} A_n^e \begin{Bmatrix}\cos(k_n x)\\ -\sin(k_n x)\end{Bmatrix} \cosh(\Gamma_1 y), & 0 < y \leqslant d_1 \\ i\sum_{n=1}^{\infty} B_n^e \begin{Bmatrix}\cos(k_n x)\\ -\sin(k_n x)\end{Bmatrix} \cosh(\Gamma_2(h-y)), & d_1 < y \leqslant d_1 + d_h \end{cases} \tag{A22}$$

where the upper and the lower terms inside the curly brackets refer to even and odd modes respectively. Under reflection in the yz plane, the symmetries of the even modes are ψ^h-odd, ψ^e-even while the odd-mode symmetries are ψ^h-even, ψ^e-odd. All field components can be expressed in terms of ψ^h are ψ^e [15]. The x and y dependences are chosen so that the tangential components of $\boldsymbol{E}$ and the normal components of $\boldsymbol{H}$ vanish on the metal enclosure at $x = \pm a$, $y = 0, h$. For even modes $k_n = (2n-1)\pi/2a$, and for odd modes $k_n = (n-1)\pi/a$. Γ_1 and Γ_2 are given in (9).

The four coefficients A_n^h, B_n^h, A_n^e, and B_n^e can be related to the components of the strip currents by applying the interface conditions on the field components at $y = d$, namely, $E_z(x,d-) = E_z(x,d+)$, $E_x(x,d-) = E_x(x,d+)$, $H_x(x,d-) - H_x(x,d+) = J_z(x,d)$ and $H_z(x,d-) - H_z(x,d+) = -J_x(x,d)$. The symbols $d-$ and $d+$ denote, respectively, infinitesimally small distances below and above the plane $y = d_1$. Two additional conditions at $y = d_1$ on E_z and E_x which are zero within $0 < |x| \leqslant w$ and nonzero in the region $w < |x| \leqslant a$ yield (1). After lengthy but straightforward algebra, we obtain

$$\begin{aligned}
E_x &= \sum_{n=1}^{\infty} Q_{xn}^p \begin{Bmatrix}\sin(k_n x)\\ \cos(k_n x)\end{Bmatrix} \sinh(\Gamma_p y_p) \\
H_x &= \sum_{n=1}^{\infty} R_{xn}^p \begin{Bmatrix}-\cos(k_n x)\\ \sin(k_n x)\end{Bmatrix} \sinh(\Gamma_p y_p) \\
E_y &= \sum_{n=1}^{\infty} Q_{yn}^p \begin{Bmatrix}\cos(k_n x)\\ -\sin(k_n x)\end{Bmatrix} \cosh(\Gamma_p y_p) \\
H_y &= \sum_{n=1}^{\infty} R_{yn}^p \begin{Bmatrix}\sin(k_n x)\\ \cos(k_n x)\end{Bmatrix} \sinh(\Gamma_p y_p) \\
E_z &= \sum_{n=1}^{\infty} iQ_{zn}^p \begin{Bmatrix}-\cos(k_n x)\\ \sin(k_n x)\end{Bmatrix} \sinh(\Gamma_p y_p) \\
H_z &= -\sum_{n=1}^{\infty} iR_{zn}^p \begin{Bmatrix}\sin(k_n x)\\ \cos(k_n x)\end{Bmatrix} \cosh(\Gamma_p y_p)
\end{aligned} \tag{A23}$$

where $p = 1,2$ refer to regions 1 and 2, respectively, and $y_1 = y$, $y_2 = h - y$. The coefficients Q_{qn}^p for the electric field components are given by

$$\begin{aligned}
Q_{xn}^p &= Z_0\hat{A}\left(\bar{Z}_{xx}\bar{J}_{xn} \pm \bar{Z}_{xz}\bar{J}_{zn}\right)/\sinh(\Gamma_p d_p) \\
Q_{yn}^p &= (-1)^p Z_0\hat{A}\bar{Z}_e\left(k_n\bar{J}_{xn} \pm \beta\bar{J}_{zn}\right)/\left(\Gamma_p \sinh(\Gamma_p d_p)\right) \\
Q_{zn}^p &= -Z_0\hat{A}\left(\bar{Z}_{zx}\bar{J}_{xn} \pm \bar{Z}_{zz}\bar{J}_{zn}\right)/\sinh(\Gamma_p d_p)
\end{aligned} \tag{A24}$$

where $\bar{Z}_{ij} = Z_{ij}/Z_0$ are the normalized forms of the impedances defined in (3)–(6). Similarly, for the magnetic field components,

$$\begin{aligned}
R_{xn}^p &= (-1)^p\Gamma_p\hat{A}\left(\hat{Z}_{zx}^p\bar{J}_{xn} \pm \hat{Z}_{zz}^p\bar{J}_{zn}\right)/\left(k_0 \sinh(\Gamma_p d_p)\right) \\
R_{yn}^p &= \hat{A}\bar{Z}_h\left(-\beta\bar{J}_{xn} \pm k_n\bar{J}_{zn}\right)/\left(k_0 \sinh(\Gamma_p d_p)\right) \\
R_{zn}^p &= (-1)^p\Gamma_p\hat{A}\left(\hat{Z}_{xx}^p\bar{J}_{xn} \pm \hat{Z}_{xz}^p\bar{J}_{zn}\right)/\left(k_0 \sinh(\Gamma_p d_p)\right)
\end{aligned} \tag{A25}$$

with

$$\hat{Z}_{xx}^{p} = \left(\alpha_{nx}^2 \frac{k_{0p}^2}{\Gamma_p^2} \bar{Z}_e + \alpha_{nz}^2 \bar{Z}_h \right)$$

$$\hat{Z}_{zz}^{p} = \left(\alpha_{nz}^2 \frac{k_{0p}^2}{\Gamma_p^2} \bar{Z}_e + \alpha_{nx}^2 \bar{Z}_h \right)$$

$$\hat{Z}_{xz}^{p} = \hat{Z}_{zx}^{p} = \alpha_{nx}\alpha_{nz} \left(\frac{k_{0p}^2}{\Gamma_p^2} \bar{Z}_e - \hat{Z}_h \right) \qquad \text{(A26)}$$

where $k_{01}^2 = \epsilon_r k_0^2$, $k_{02}^2 = k_0^2$, $\alpha_{nx} = k_n / \{k_n^2 + \beta^2\}^{1/2}$, and $\alpha_{nz} = \beta / \{k_n^2 + \beta^2\}^{1/2}$. As before, the upper (lower) sign in (A24) and (A25) refers to even (odd) modes. To obtain the contribution to $\boldsymbol{E}$ or $\boldsymbol{H}$ from the current in the jth strip only, we have to replace $\bar{J}_{xn}$ and $\bar{J}_{zn}$ in (A24) and (A25) by $\bar{J}_{x,j}(n)$ and $\bar{J}_{z,j}(n)$, respectively, from (A19) and (A20).

Acknowledgment

The authors are very grateful to Dr. D. C. Webb and Dr. H. S. Newman for many helpful discussions.

References

[1] R. W. Simon *et al.*, "Low-loss substrate for epitaxial growth of high-temperature superconductor thin film," *Appl. Phys. Lett.*, vol. 53, pp. 2677–2679, 1988.

[2] D. E. Oates, A. C. Anderson, and B. S. Shih, "Superconducting stripline resonators and high-T_c materials," in *IEEE MTT-S Int. Microwave Symp. Dig.*, 1988, pp. 418–420.

[3] R. L. Sandstrom *et al.*, "Lanthanum gallate substrates for epitaxial high-temperature superconducting thin films," *Appl. Phys. Lett.*, vol. 53, pp. 1874–1876, 1988.

[4] G. Keren, A. Gupta, F. A. Geiss, A. Segmuller, and R. B. Laibowitz, "Epitaxial films of $YBa_2Cu_3O_{7-\delta}$ on $NdGaO_3$ and $SrTiO_3$ substrates deposited by laser ablation," *Appl. Phys. Lett.*, vol. 54, pp. 1054–1056, 1989.

[5] R. R. Bonetti and A. E. Williams, "Preliminary design steps for thin film superconducting filters," in *IEEE MTT-S Int. Microwave Symp. Dig.*, 1990, pp. 273–276.

[6] T. Itoh and R. Mittra, "Spectral domain approach for calculating the dispersion characteristics of microstrip lines," *IEEE Trans. Microwave Theory Tech.*, vol. MTT-21, pp. 496–499, 1973.

[7] T. Itoh and R. Mittra, "A technique for computing dispersion characteristics of shielded microstrip lines," *IEEE Trans. Microwave Theory Tech.*, vol. MTT-22, pp. 896–898, 1974.

[8] R. H. Jansen, "Unified user-oriented computation of shielded, covered and open microwave and millimeter-wave transmission-line characteristics," *Microwave, Optics, and Acoustics*, vol. 3, pp. 14–22, 1979.

[9] R. H. Jansen and M. Kirschning, "Arguments and an accurate model for the power–current formulation of microstrip characteristic impedance," *Arch. Elek. Übertragung.*, vol. 37, nos. 3/4, pp. 108–112, 1983.

[10] W. J. Getsinger, "Measurement and modeling of the apparent characteristic impedance of micropstrip," *IEEE Trans. Microwave Theory Tech.*, vol. MTT-31, pp. 624–632, 1983.

[11] J. R. Brews, "Characteristic impedance of microstrip lines," *IEEE Trans. Microwave Theory Tech.*, vol. MTT-35, pp. 30–34, 1986.

[12] N. Fache and D. Zutter, "Circuit parameters for single and coupled microstrip lines by a rigorous full-wave space-domain analysis," *IEEE Trans. Microwave Theory Tech.*, vol. 37, pp. 421–425, 1989.

[13] A. A. Mostafa, C. M. Krowne, and K. A. Zaki, "Numerical spectral matrix method for propagation in general layered media: Application to isotropic and anisotropic substrates," *IEEE Trans. Microwave Theory Tech.*, vol. MTT-35, pp. 1399–1467, 1987.

[14] C. M. Krowne, A. A. Mostafa, and K. A. Zaki, "Slot and microstrip guiding structures using magnetoplasmas for nonreciprocal millimeter-wave propagation," *IEEE Trans. Microwave Theory Tech.*, vol. 36, pp. 1850–1860, 1988.

[15] R. Harrington, *Time Harmonic Electromagnetic Fields*. New York: McGraw-Hill, 1961, pp. 158–163.

Achintya K. Ganguly received the Ph.D. degree in physics from New York University, New York, NY, in 1965.

At New York University (1965–1972), he worked on the theory of light scattering from quasiparticles in solids. From 1967 to 1972, he was a staff member at GTE Laboratories and worked on electron–phonon interaction in solids and surface acoustic wave propagation in piezoelectric materials. He joined the Naval Research Laboratory in 1972 as a Research Physicist. At NRL, he worked on magnetostatic and magnetoelastic surface wave propagation and cyclotron resonance in a 2-D electron gas system. At present, he is working on problems related to high-power microwave generation by the interaction of relativistic electron beams and electromagnetic radiation in devices such as the gyrotron and ubitron/FEL.

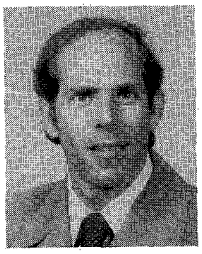

Clifford M. Krowne (S'73–M'74–SM'84) attended the University of California, Berkeley, and received the B.S. degree in physics from the University of California, Davis, in 1970 and the M.S. and Ph.D. degrees in electrical engineering from the University of California, Los Angeles, in 1972 and 1975, respectively.

In 1970, he was employed in the Microelectronics Division of Lockheed Missiles and Space Company. In 1976 he joined the technical staff of the Watkins–Johnson Company in Palo Alto, CA, and in 1978 he became a faculty member in the Department of Electrical Engineering at North Carolina State University, Raleigh. Since 1982, he has been with the Electronics Science and Technology Division of the Naval Research Laboratory, Washington, DC, studying microwave and millimeter-wave properties of active and passive solid-state devices. He also was an Adjunct Professor of Electrical Engineering at the University of Maryland, College Park, MD.

Dr. Krowne has published more than 90 technical papers on solid-state electronics, microwave circuits, electromagnetics, engineering education, and applied physics. He has served on the technical program conference committees of the Antennas and Propagation Society and the Microwave Theory and Techniques Society and has chaired sessions in the electromagnetic theory, microstrip antenna, and solid-state devices/circuits areas. Dr. Krowne was a member of the 1987 MTT Symposium steering committee. He is a member of Phi Kappa Phi and Tau Beta Pi.